

Hyperspectral Imaging to Discern Malignant and Benign Canine Mammary Tumors

**A Thesis Proposal
Submitted to the
Temple University Graduate Board**

**In Partial Fulfillment
of the requirements for the Degree
Masters of Science in Electrical Engineering**

**By
Amrita Sahu
December 2012**

**Dr. Chang-Hee Won
Thesis Advisor**

**Dr. Nancy Pleshko
Committee Member**

**Dr. Joseph Picone
Committee Member**

Abstract

Hyperspectral imaging is an emerging technology in the field of biomedical engineering which may be used as a non-invasive modality for cancer characterization. In this project, we propose to investigate near-infrared (NIR) hyperspectral imaging for the characterization of canine mammary cancer. Near-infrared hyperspectral imaging has been used for the detection of various kinds of human cancer; breast, gastric, prostate and tongue. A research group has also investigated the use of NIR reflectance imaging to detect canine cancer using fluorescent dyes. The use of NIR hyperspectral imaging, however, has been limited for the characterization of canine cancer. In this project, we have already acquired hyperspectral images of 22 canine mammary tumors. Preliminary results of 2 canine patients show that the spectra of canine cancer tissue differ from those of benign tissue. The malignant tissue has relatively low reflectance intensity compared to the benign tissue; in the wavelength range between 650nm to 1100nm. The decreased reflectance intensity observed for malignant tumors is due to the increased microvasculature and therefore higher blood content of cancerous tissue relative to benign tissue. In the future, we will normalize and preprocess the spectral dataset. We propose to apply various algorithms such as Support Vector Machine, Linear Discriminant Analysis, Principal Component Analysis and Tissue Optical Methods on the spectral data to discern the malignant and benign tumors. The advantage of cancer detection using hyperspectral imaging is that it is non-invasive and less time consuming than traditional methods like biopsy.

Keywords: Hyperspectral imaging, canine mammary tumor, near-infrared spectroscopy, tumor characterization

Table of Content

List of Figures

1. Introduction.....	1
1.1 Motivation.....	1
1.2 Statement of Problem.....	2
1.3 Research Objectives.....	2
1.4 Organization of Thesis Proposal.....	3
2. Background.....	3
2.1 Infrared Hyperspectral Imaging.....	3-5
2.2 Cancer Detection Using Infrared Hyperspectral Imaging.....	6
2.2.1 Prostate Cancer Detection.....	6-7
2.2.2 Tongue Cancer Detection.....	7-8
2.2.3 Gastric Cancer Detection.....	8-9
2.2.4 Breast Cancer Detection.....	9-10
2.2.5 Skin Cancer Detection.....	10
2.3 Other diseases diagnosed by Hyperspectral Imaging.....	11
3. Experimental Setup and Data Acquisition.....	12
3.1 Hyperspectral Imaging System Description.....	12
3.2 Method of Data Acquisition from Canine patients.....	13-14
4. Normalizing and Preprocessing of data.....	15
4.1 Normalization Using Standard Reflectance Standards.....	15
4.2 Other normalization methods used in NIR Imaging.....	16
4.3 Derivative Methods and its applications.....	17
5. Data Analysis.....	17
5.1 Support Vector Machine.....	17-19
5.2 Linear Discriminant Analysis.....	19-21
5.3 Principal Component Analysis.....	21
5.4 Tissue Optical Indices Method.....	21-22
6. Preliminary Results.....	22-23
7. Discussion.....	23-25
8. Future Research Plan.....	25-26

References

List of Figures

Figure 1: Needle biopsy for breast cancer.....	1
Figure 2: A hyperspectral three dimensional imaging cube	4
Figure 3: A hyperspectral imaging setup for tissue analysis.....	5
Figure 4a: Detection of prostate cancer tissue (green area) using the classification method	6
Figure 4b: In-vivo spectral signature of benign and malignant lesion.	6
Figure 5: The hyperspectral imaging setup used by the authors for the gastric cancer experiment.....	8
Figure 6: Schematic view of the hyperspectral imaging acquisition system.....	13
Figure 7: The canine patient with multiple mammary tumors held by the doctor as.....	14
images are being captured by the hyperspectral system	
Figure 8a: The hyperspectral image of canine mammary tumors.....	14
Figure 8b: The digital image of canine mammary tumors.....	14
Figure 9: The reflectance spectra of canine patient Kiki.....	22
Figure 10: The reflectance spectra of canine patient Tinkerbelle.....	23
Figure 11: The 500W quartz tungsten halogen lamp used in the canine experiment.....	24
Figure 12: The 300W Sunbeam Xenon Lightsource	24

1. Introduction

1.1 Motivation

Mammary tumor or neoplasm originates in the mammary gland. The frequency of mammary neoplasia varies highly across different species. For example, among domestic species, dog has the highest prevalence of mammary neoplasia which is approximately three times higher than that of women [1]. The frequency of malignant mammary tumor also varies across species. In dogs, approximately 50% of all mammary gland tumors are malignant or cancerous and have the potential for metastasis whereas in cats the figure is approximately 90% [2]. Once a tumor reaches metastatic stage, the chances of successful treatment become very low. Therefore, early detection of malignant tumors is necessary for successful treatment of cancer. Currently, biopsy is the gold standard for cancer diagnosis, which involves removal of tissue from the mammary tumor, and then be examined by a pathologist. It is invasive, expensive and requires highly trained surgeons and pathologists. The results require several days to be prepared and therefore the technique is time consuming. Moreover, in a biopsy, the whole tumor is not analyzed, only a few tissue samples from the tumor are taken. To avoid the above disadvantages, we develop a portable hyperspectral imaging system for characterizing canine mammary tumors.

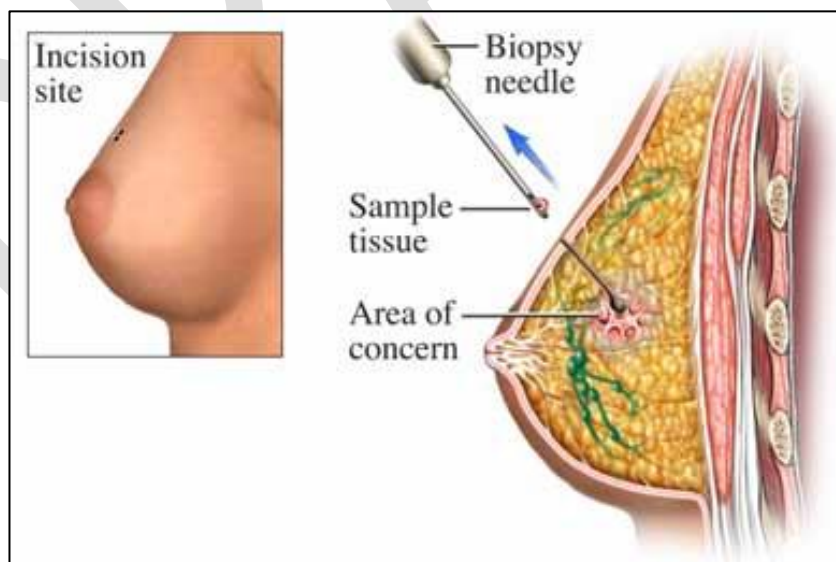


Figure 1: Needle biopsy for breast cancer. The method is invasive and time-consuming

Recently, hyperspectral imaging is an emerging technology in the field of biomedical engineering which may be used as a non-invasive modality for cancer characterization. For example, using hyperspectral imaging (HSI), prostate cancer has been detected with 92.8% sensitivity and 96.9% specificity [3]. Also cancers like gastric cancer [4] and tongue cancer [5] has been detected using hyperspectral imaging. For tongue cancer, the authors in [5] obtain 96.5% recognition rate. HSI was used by Medina for the characterization of iris reflectance to non-invasively diagnose ocular diseases [6] and by Panasyuk for the detection of tumor and normal breast tissues [7]. This imaging technology has also been used for the detection and analysis of intestinal ischemia [8], diagnose hemorrhage shock [9], detection and characterization of emphysema from healthy lung tissue [10] and in-vivo detection and grading of cervical precancers and of pigmented skin lesions [11].

Hyperspectral imaging is capable of providing both the spectral and spatial information of tissues over hundred or more spectral bands. So it extends invisible wavelength regions to human vision range. Thus hyperspectral imaging may aid a surgery, and allow the assessment of tissue continuously without interrupting surgery. Thus, it can be used as a virtual biopsy [3]. So HSI is non-invasive less time-consuming. In this project, near infrared hyperspectral imaging will be used for canine cancer characterization.

1.2 Statement of Problem

The ultimate goal of this project is to discern benign and malignant canine mammary cancer by near-infrared hyperspectral imaging.

1.3 Research Objectives

The research objectives of this project are:

- a) Conduct a thorough literature search on cancer detection using hyperspectral imaging.
- b) Design an experiment to acquire the hyperspectral images of the canine mammary tumors from the canine patients
- c) Find the best normalization and preprocessing techniques to normalize the spectra.
- d) Develop an algorithm to discern the malignant tumors from the benign tumors.

1.4 Organization of Thesis Proposal

This thesis proposal document is organized as follows. A background is given in order to lay the foundation for this work. The concept of infrared hyperspectral imaging is described. Then cancer detection using hyperspectral imaging is introduced. The method of breast, gastric, prostate, skin and tongue cancer characterization using hyperspectral imaging is described. Following the background section, the experimental setup and data acquisition method is detailed. Normalization of the spectral data is very important for data analysis. So the normalization and other preprocessing techniques are described, followed by the different types of algorithms which will be tried out on the canine spectral data to discern malignant and benign canine mammary tumors. Preliminary results are shown thereafter, followed by the Discussion section, where different issues faced during the project are discussed. Finally the proposal document ends with a detailed research plan.

2. Background

2.1 Infrared Hyperspectral Imaging

Conventional color cameras acquire intensity information from the visible electromagnetic spectrum, that is, red, green and blue. Hyperspectral imaging measures and collects intensity information over more than hundred spectral bands across the electromagnetic spectrum. So it extends invisible wavelength regions to human vision range. Hyperspectral images are acquired by 'hyperspectral sensors' and these sensors have a variety of applications in the fields of agriculture, physics, remote sensing and surveillance. This technique was used originally for the purpose of remote sensing, and that project was initiated and developed by NASA [12]. But recently, hyperspectral imaging is also being used in the field of medicine, particularly cancer detection. This is because this kind of novel technology can quantify several biomarkers found in tissue, and thereby can be used for non-invasive tissue analysis.

During hyperspectral imaging, the data produced by the sensor consists of a collection of images. This set of images can be represented by a three dimensional cube of image, where the first two coordinates represent the spatial coordinate of a pixel and the third coordinate gives the wavelength of a particular spectral band. Thus it gives both the spectral and spatial information at the same time. The accuracy of these sensors is measured in terms of two parameters: spatial resolution and spectral resolution. Spectral resolution is the width of each band of the spectrum and is given by $\Delta\lambda$, where $\Delta\lambda$ is the minimum

wavelength difference that can be distinguished at a wavelength λ . Spatial resolution is the measure of how closely we can resolve lines in an image, and is given by the number of pixel values per unit length.

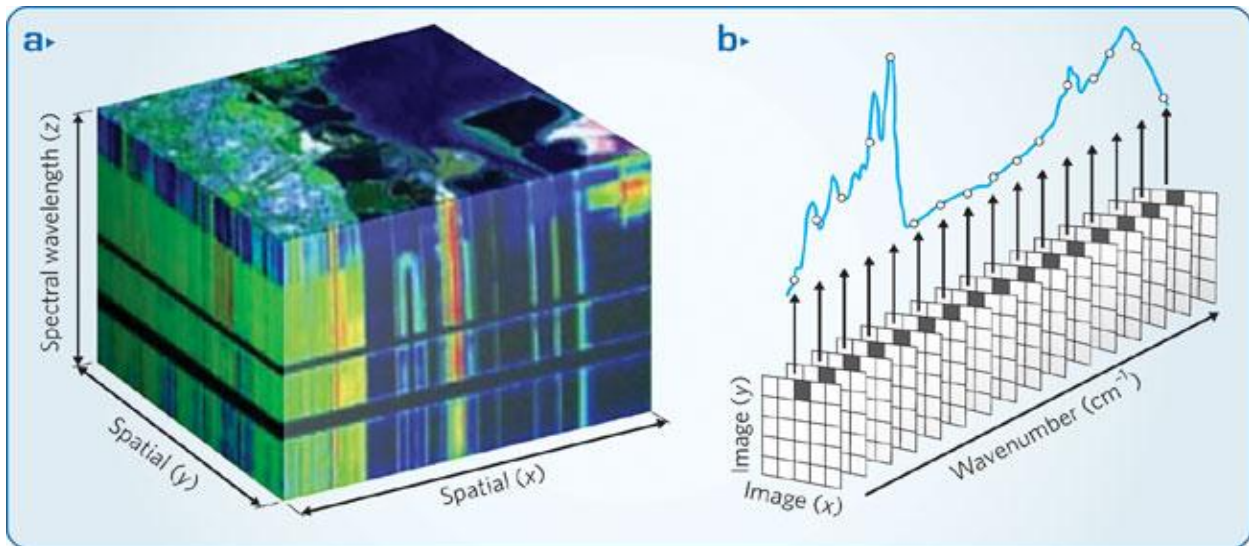


Figure 2: A hyperspectral three dimensional imaging cube where the three coordinates represent the horizontal axis, vertical axis and the wavelength respectively.

There are three different kinds of hyperspectral imaging techniques. The first kind used a prism or a grating as the dispersive medium in the optical system, the second class uses band pass filter, which can be tunable or fixed, and the third class implements a technique called the Fourier Transform Spectroscopy. In this technique, Fourier Transform is applied to obtain the spectral decomposition of the light entering the hyperspectral sensor. In this project, the second class of hyperspectral imaging technique will be used. Our hyperspectral camera consists of a liquid crystal tunable filter, which scans the spectrum in increment of 10 nm.

Hyperspectral Imaging has a wide array of applications in many fields. Primarily, it was developed by NASA for the purpose of remote sensing, geology mining and space exploration. Recently, it is also being used in agriculture, mineralogy, surveillance, physics, chemical imaging and non-invasive tissue analysis for detection of cancer and other diseases. In agriculture, this technology is used to monitor the health of crops and to detect chemical composition, nutrient and water status and disease outbreak for plants. Hyperspectral imaging is used for obtaining the spectral signatures of geological samples like feldspar, silica, calcite groups to differentiate the minerals of interest from the surrounding region. Some minerals like gold and diamond are also identified from hyperspectral airborne images. Hyperspectral surveillance

is used for military purposes, and it is able to detect the presence of opposition even if countermeasures are taken to avoid airborne surveillance. Nowadays, hyperspectral camera which incorporates thermal infrared imaging are used for this purpose. Chemical Imaging is another application for which hyperspectral imaging is used. At war, soldiers are exposed to chemical agents and harmful plumes which are difficult to detect. But using hyperspectral imaging, detection and identification of such harmful chemicals have now become possible. This technology is also used in many countries for the continuous monitoring of oil drills. If oil leaks from the oil drill, it could cause extensive damage to the ecosystem. So hyperspectral sensors can be deployed to build detection and warning system for oil drills .

In this project, we will focus on the use of hyperspectral imaging for non-invasive canine cancer detection. Near-infrared hyperspectral imaging has been used for the detection of various kinds of cancer; breast, gastric, prostate, tongue. In this project, we focus on the near-infrared region (NIR) that extends from 650nm to 1100nm. This is because NIR light is absorbed by certain chromophores that are biochemically significant, namely, hemoglobin, water and lipid. Thus using NIR spectroscopy, we can quantify the concentration of these important biomarkers. Literature shows that NIR light penetrates into tissue farther than light in any other spectrum, because tissue has low absorptivity in this region. Thus weakly absorbed NIR light that can penetrate several centimeters is used for the hyperspectral imaging of thick tissue such as brain, breast and muscle [19]. Literature shows some favorable results in the detection of breast cancer using NIR spectroscopy. Since canine mammary tumor is physiologically similar to human breast tumor, we use NIR spectral range (650-1100nm) as the light transmission range for our project.

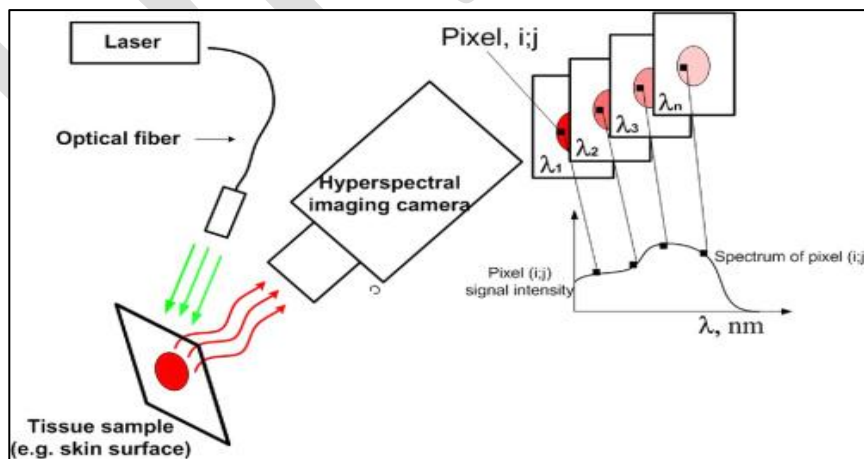


Figure 3: A hyperspectral imaging setup for tissue analysis. In our experiment we will use halogen tungsten light instead of laser

2.2 Cancer Detection Using Infrared Hyperspectral Imaging

2.2.1 Prostate Cancer Detection

Devising non-invasive techniques for early detection of cancer has now become a promising field in the area of biomedical engineering and medical science. Paper by Akbari *et al.* [3] describes a non-invasive detection method of prostate cancer cell in mice using hyperspectral image processing and machine learning techniques.

Using least square support vector machines, the authors classify the hyper spectral images of the cancerous and normal tissue. They also indicate the differences of reflectance properties in cancer and normal tissue using spatially resolved images. The experiment is carried out on diseased mice (in-vivo) as well as on pathological slides (in-vitro).

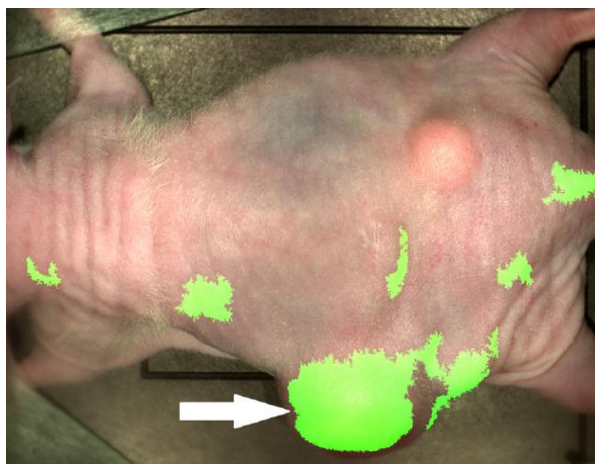


Figure 4a: Detection of prostate cancer tissue (green area) using the classification method with least square support vector machine.

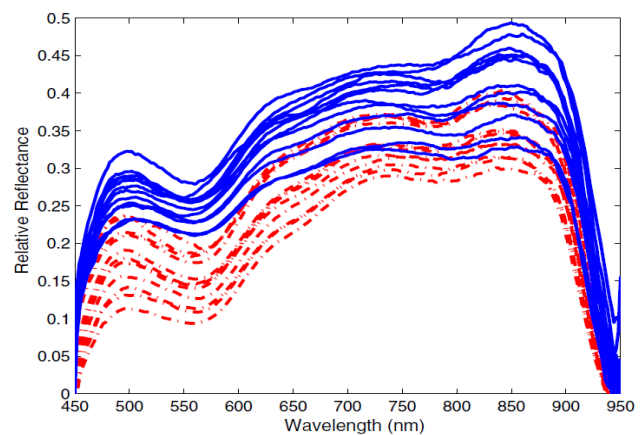


Figure 4b: In-vivo spectral signature of benign and malignant lesion. The dashed red lines represent the malignant lesion and the continuous line represents the benign regions.

To remove the spectral non-uniformity of illumination device, the authors use a normalization technique. The technique is to minimize the influence of dark current. To solve the classification problem, the authors employ least square support vector machine in which we solve a linear equation (instead of quadratic programming) in high dimensional space or kernel space. In any least square method, we aim to minimize the sum of the square of the error.

The authors evaluate the classification technique using two parameters: sensitivity and specificity. Sensitivity measures the percentage of correctly identified tumor tissue and specificity measures the percentage of healthy tissue correctly identified. The results show the specificity of the classification technique is 92.8% (with a margin of 2.0%) and sensitivity of 96.9 % (with a margin of 1.3%) for 11 mice [3].

The method describe above is superior to conventional methods like tissue biopsy because it measures spectra of tissue point by point. It also spectrally and spatially verifies the spectral variations of different types of tissue. Therefore, it is a continuous non-intervening evaluation technique for suspicious cancer tissues and can be used as a virtual biopsy [3].

2.2.2 Tongue Cancer Detection

The paper by Liu [5], describes tongue cancer detection using hyperspectral imaging. The reflectance spectra dataset of 34 tongue tumors were collected using an acousto-optic tunable filter (AOTF) and a spectral adapter. For medical applications, most hyperspectral systems use tunable filters rather than spatial scanning, because they do not need mechanically moving part and are faster. AOTF is a solid state tunable filter and is based on the principle of acoustic diffraction of light in an anisotropic medium. They are advantageous over other spectrometers, because they are not sensitive to mechanical shock or vibration. AOTF technology also provides wider tuning range, more field of view, and can be easily programmed. For illumination purposes, the authors have used 500W halogen lamps. Noise is present in the tumor spectral data because of the saliva on the tongue and its instinctive squirming. For denoising, the authors used median filters. To remove the spectral non-uniformity, a normalization procedure has been used using standard reflectance boards.

Sparse representation (SR) has been used as the classification algorithm to detect the cancerous tongue tumors. Sparse signal representation has been proven to be an extremely powerful computer vision tool for representing high dimensional signals [5]. This is because some classes of signals have naturally occurring sparse properties. The authors have first shown the difference in the spectral properties of the tumor and normal tissue. The SR classifier was used to develop an algorithm to detect the cancerous pixels from the non-cancerous pixels. The authors achieved a recognition rate of 96.5%.

To prove that SR algorithm is computationally superior to traditional hyperspectral algorithms like support vector machine (SVM) or relevance vector machine (RVM), the authors have compared the performance of the SR algorithm to that of the SVM and RVM. The SR method worked better than the other two even when the tumors were less than 3mm deep and was covered with mucosa. The authors

have also shown that the classification time for their method is less than SVM and RVM. The false negative rate (FNR) and the false positive rate (FPR) were calculated for each hyperspectral image. The SR method showed a FNR and FPR of 6.3% and 8.7% respectively [5].

Thus this method shows promise in the detection of tongue cancer using hyperspectral imaging and sparse representation. This computer aided tool can help the doctors decide non-invasively as to whether a patient has tongue cancer.

2.2.3 Gastric Cancer Detection

The paper by Akbari [4] describes gastric cancer detection using infrared hyperspectral imaging. Gastric tumors were imaged from 10 human subjects and the results were correlated with the histopathology results. A total of 101 images were taken from the 10 patients. So each sample was imaged 10 times, to ensure repeatability of the system. The NIR spectral range of 1000-2500 nm was used for this project. The hyperspectral imaging device was a tunable optical band pass filter, and the spectral resolution of the camera was 6.29 nm. The light source for illumination consisted of two 150W halogen lamps, with diffuse reflectors. In this experimental setup, the camera was attached to a frame and the frame was fixed. The frame was controlled by a linear actuator. This made sure that the distance between the lens and the sample is constant. This is a very important factor that should be kept in mind while designing our canine experiment.

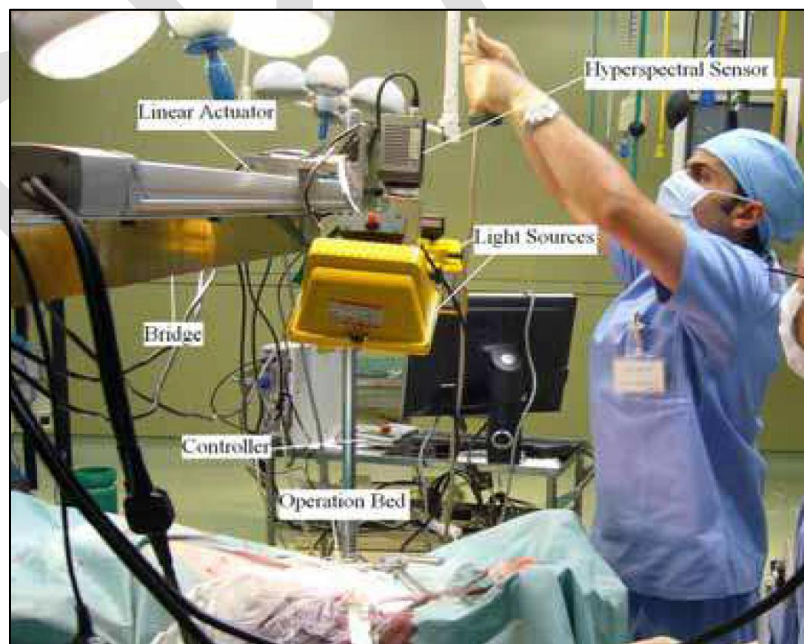


Figure 5: The hyperspectral imaging setup used by the authors for the gastric cancer experiment

In this paper, the authors have normalized the data using standard reflectance boards. The noise was removed by median filtering. The differences in the spectral characteristics of the tumor and the normal tissue have been shown. The standard deviation of the spectral signature of the tumors is higher compared to the normal tissue. Four different classification methods, the support vector machine (SVM), standard deviation (SD) method, integral method and the normalized difference cancer index (NDCI) method were used to detect the cancerous tumors. Out of these four algorithms, NDCI gave the best results. Using this method, the authors obtained a sensitivity and specificity of 93% and 91% respectively [4].

The above proposed method shows potential in the non-invasive detection of gastric cancer. This method could detect tumors less than 0.5mm in size [4]. Also, determining the tumor bed during surgery is also challenging for the doctors. Such imaging technology can be used to determine the tumor bed during surgery and also to ensure that the entire tumor has been removed after tumor resection. This it can help in the segmentation of tumors and remove ambiguity between the malignant and benign regions.

2.2.4 Breast Cancer Detection

Diffuse optical spectroscopy using the near-infrared light spectrum has been investigated for the detection and clinical management of breast cancer [13] [14]. In these papers, instrumentation consists of a broadband steady-state spectrometer system (650-1100nm) and a six wavelength frequency domain instrument which consists of six laser diodes (661, 686, 786, 808, 822, and 852 nm). A fiber optic cable delivers the laser light to the tissue. A hand held probe which consists of an avalanche photodiode detector, records the diffused light signals from the tissue. Although this system is different from the hyperspectral imaging setups used in the previous papers, the principle is the same; they investigate non-invasive tissue analysis using laser scanners and NIR light.

Currently, the most common non-invasive procedure for breast cancer screening is mammography; however this method suffers from low sensitivity and specificity and does not work well for dense breast masses. Because of these disadvantages, many research groups have tried to use optical methods for breast cancer screening. Optical methods are non-invasive, less time-consuming, do not use ionizing radiation and is less expensive. In these papers, the authors have used NIR laser diodes to enhance physiological and biochemical contrast between the malignant and normal breast tissues.

Paper by Cerussi [15] presents the clinical results from 58 malignant breast tumors. Physiological properties like hemoglobin, water and lipid content was significantly different between malignant and normal breast tumors. Malignant tumors showed higher concentration of deoxy-hemoglobin, oxy-

hemoglobin and water and lower contents of tissue lipid compared to normal tissue. A tissue optical index was defined which increased the contrast between the malignant and normal tissue.

$$TOI = \frac{[H_2O][HbT]}{[Lipid][StO_2]}$$

These measurements have underlying physiological meaning: Higher content of hemoglobin (HbT) suggests elevated tissue volume and angiogenesis; higher water content (H₂O) suggest edema and increased cellularity, decreased StO₂ indicated tissue hypoxia (a pathological condition in which tissue is deprived of adequate oxygen supply) driven by metabolically active tumor cells, decreased lipid content [Lipid] reflects displacement of parenchymal adipose. A higher TOI suggest that the tumor is malignant, because it indicates higher metabolic activity of the cells [14].

Also, an important application of the above proposed method is monitoring the response of patients to cancer therapies. One of the cancer therapy methods for women in advanced stages of breast cancer is pre-surgical chemotherapy, which can shrink tumors to a smaller size, so that they can be operated and surgically removed. In order to maximize the therapeutic effectiveness, the above proposed non-invasive optical method can be used to examine and assess the physiological properties of the tumor.

2.2.5 Skin Cancer Detection

Skin cancer is a common form of cancer and more than a million people are annually affected by this form of cancer in the United States. Dermatologists identify skin melanomas, but biopsy is required for definitive evaluation. But biopsy is not feasible for a patient with a large number of melanomas. Therefore, a non-invasive method to detect skin cancer in place of the traditional biopsy is in great demand.

The paper by Zeng [16] describes a method of skin cancer detection using Raman spectroscopy. In this paper, the authors develop a clinical research prototype that can obtain Raman spectra from skin in vivo within 1 second. The imaging instrument consists of a diode laser (785 nm), a spectrograph, a CCD detector and Raman optical probe. The probe was designed in such a way that the collection of Raman signals is maximum. In order to process the raw spectral data, a polynomial fitting algorithm was used to remove the background fluorescence. Data from 274 skin lesion were analyzed which included cancers, precancerous tumors and benign lesions. Using Raman spectroscopy, the authors obtained sensitivity and specificity of 90% and 75%.

2.2.6 Canine Mammary Tumor Detection

In the paper by Gurfinkel [21], fluorescent dyes have been used to discern canine adenocarcinoma from normal tissue. Two fluorescent dyes: indocyanine green (ICG) and carotene-conjugated 2-devinyl-2-(1-hexyloxyethyl) pyropheophorbide (HPPH-car) were administered intravenously in the canine patient. For illumination of the tissue, a 660 nm laser diode beam was used. The fluorescence generated by the dyes upon propagating to the tissue surface, is captured by a CCD camera. The uptake and release rates of the dye were studied and they varied considerably in the diseased and normal tissue. Pharmacokinetic model was used to monitor the delivery of the dyes.

2.3 Other diseases diagnosed by Hyperspectral Imaging

Hyperspectral imaging has also been used to detect diseases such as intestinal ischemia and lung emphysema [17] [10]. Paper by Akbari [17] describes the detection of intestinal ischemia using hyperspectral imaging both in the visible and the invisible wavelength range. Intestinal Ischemia is caused by the insufficient flow of oxygenated blood to the intestine, which may result in bloody diarrhea, gangrene and other infection. The spectral signatures of the intestinal ischemic region of a pig's intestine were extracted using two hyperspectral imagers (400-1000nm and 900-1700nm). Two filters were designed as the classification algorithm and the results were compared with that of the traditional support vector machine (SVM) method. One of the filter classification method could detect ischemic tissue from normal intestinal tissue and other organs with a FPR (False Positive Rate) and FNR (False Negative Rate) of 1% and 1% respectively. The SVM method gave a FPR and FNR of 5% and 6% respectively.

The paper by Jong-Ha Lee [10] describes the characterization of emphysema from healthy tissue using hyperspectral imaging. The NIR spectral range of 650nm to 1100nm was used. Peak absorption intensity was observed at four wavelengths (760, 805, 915, and 970 nm), which is characteristic of the four tissue chromophores. Spectral signatures from the normal pig's lung phantom and the smoker's lung phantom were extracted and compared. The reflectance intensity of the smoker's lung tissue was considerably higher than the normal lung tissue over the entire wavelength range (650-1100nm). This information could be useful for detecting lung emphysema from healthy lung tissue.

3. Experimental Setup and Data Acquisition

In this section, the hyperspectral imaging system will be described. Also, the method of acquiring hyperspectral images of the canine mammary tumors from the canine patients will be described.

3.1 Hyperspectral Imaging System Description

To capture the hyperspectral imaging data, a portable hyperspectral tunable imaging system was used. It consists of digital imager (Qimaging Inc., Surrey, British Columbia), a Liquid Crystal Tunable Filter (LCTF Cambridge Research & Instrumentation Inc., Massachusetts), and LCTF controller. The digital imager was a 1.4 megapixel, mono-cooled CCD (charged coupled device) camera; with a cell size of $6.45 \mu\text{m} \times 6.45 \mu\text{m}$ and 12 bit output. The filter is placed in front of the digital imager and has a transmission wavelength range between 650 to 1100nm with a 10nm increment. While capturing the image, the distance between the lens and the sample to be imaged should be constant. And care should be taken that the light falls as uniformly as possible on the subject.

The LCTF controller synchronizes between digital imager and LCTF. It also varies the programmed sequential bands of filter. The tuning speed of the filter is between 50 ms to 150 ms. During acquisition of the images, dual 500W quartz tungsten halogen lamps have been used for illumination. An Apple Macbook Pro laptop computer is used for the spectral image acquisition purposes. The image is visualized and the spectral signature is plotted using ENVI software (Ver. 4.5, ITT Visual information solutions, Boulder, CO) and 'The Unscrambler' version 10.1 (CAMO Software AS, Oslo, Norway) . Figure 1 shows the proposed HSI system setup.

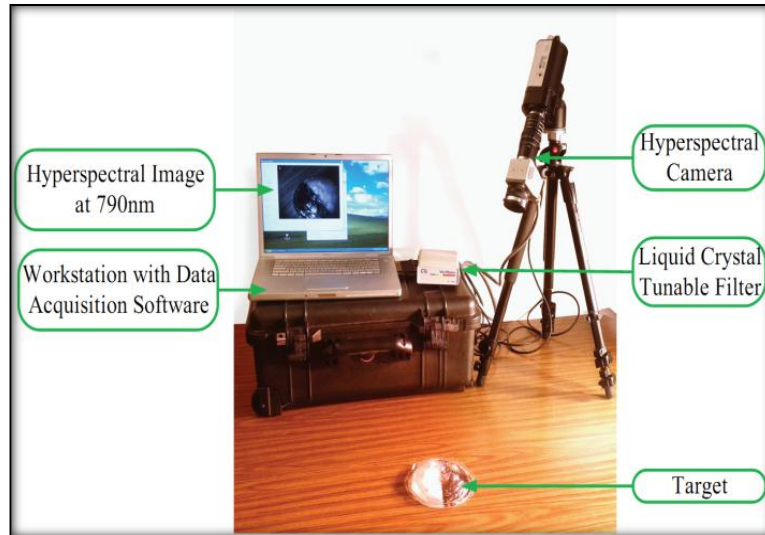


Figure 6: Schematic view of the hyperspectral imaging acquisition system. The LCTF and the computer are connected by a firewire (1394) cable. The camera and the controller are connected by a USB cable. To connect the LCTF controller and the camera, a parallel port cable has been used.

3.2 Data Acquisition from canine patients

The data was acquired in collaboration with the University of Pennsylvania Veterinary Hospital. These canine patients had multiple mammary tumors in their abdomen. The animal experiments were approved by the University of Pennsylvania IACUC Protocol #803829. In this study, the hyperspectral imaging experiment was performed on 9 dogs. Prior to image acquisition, the tumors were marked with a black marker, so that it would be easier to recognize the tumor during image analysis. During image acquisition, the dogs were held by the veterinary doctor. Each dog had to undergo biopsy to detect the malignancy of the tumors. The histopathology results were compared with our imaging analysis results. Figure 2 shows a canine patient with multiple mammary tumors.



Figure 7: The canine patient with multiple mammary tumors held by the doctor as images are being captured by the hyperspectral system.

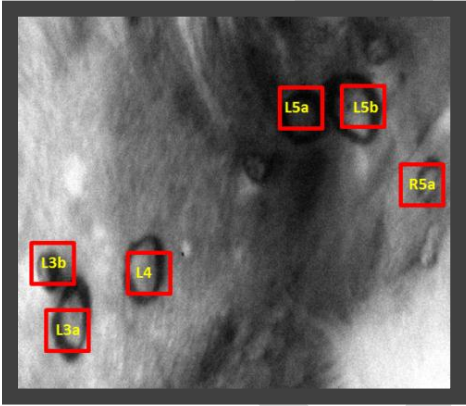


Figure 8a: The hyperspectral image of canine mammary tumors at 760nm wavelength



Figure 8b: The digital image of canine mammary tumors.

4. Normalizing and Preprocessing of data

This section describes the normalization and preprocessing techniques that will be investigated. In the first section, data normalization using standard reflectance boards will be described. This is the standard normalization procedure followed by most research groups. However, these standards were not used during our canine experiment. There are a number of normalization techniques which are available in *The Unscrambler 10.1*. These techniques are also widely used normalizing NIR data. Taking first and second derivative of the spectral data is a way of preprocessing the data to correct the baseline effects. Derivative methods and their applications are also discussed in this section.

4.1 Data Normalization by the radiometric reflection calibration process

The captured data should be normalized to treat the spectral non-uniformity of the illumination device. The raw data changes due to several factors like illumination conditions, temperature and non-uniform contour of the subject. To minimize these varying conditions, spectral data has to be normalized. The radiometric reflectance normalization process involves a pixel-to-pixel normalization of the hyperspectral image data to percentage reflectance. This is the most common approach for radiometric calibration and has been widely used [3] [4] [5]. White reference and dark current are two data that should be captured for normalization. White reference is the spectrum acquired by the hyperspectral sensor by placing the white reference board in the field of view. For this purpose, Spectralon diffuse reflectance standard SRS-99 for an approximately 99% reflectance (Labsphere Inc., Sutton, NH) should be used. The dark current is measured by taking a dark image in the absence of light. For this purpose, Spectralon diffuse reflectance standard SRS-02 for an approximately 2% reflectance (Labsphere Inc., Sutton, NH) should be used [2]. White reflectance is used to show the maximum reflectance in each wavelength. Dark current is used to address the defects by calculating the peaks in the dark current spectrum with temperature. Then the raw data is corrected using the following equation:

$$R(\lambda) = \frac{I_{raw}(\lambda) - I_{dark}(\lambda)}{I_{white}(\lambda) - I_{dark}(\lambda)}$$

Where $R(\lambda)$ is calculated reflectance value for each wavelength, $I_{raw}(\lambda)$ is the reflectance intensity of the raw data, and $I_{dark}(\lambda)$ and $I_{white}(\lambda)$ are the reflectance intensity of the 2% reflectance standard board and the 99% reflectance standard board, respectively.

4.2 Other Normalization Methods

Normalization is a family of transformations that are computed sample-wise. Its purpose is to “scale” samples in order to get all data on approximately the same scale. The following normalization methods are also used in normalizing NIR spectral data [18]:

- **Area Normalization**

This transformation normalizes a spectrum by calculating the area under the curve for the observation. The area under the curve becomes the same for all samples. It attempts to correct the transmission spectra for indeterminate path length when there is no way of measuring it.

- **Unit Vector Normalization**

This transformation normalizes sample-wise data to unit vectors. It is useful for pattern recognition applications. The normalized samples have a length (“norm”) of 1.

- **Mean Normalization**

This is the most classical case of normalization. It consists in dividing each row (each observation) of a data matrix by its average. This transformation is used in chromatography to express the results in the same units for all samples, no matter which volume was used for each of them.

- **Maximum Normalization**

This is an alternative to classical normalization which divides each row by its maximum absolute value. If all values are positive the maximum value becomes +1. If all values are negative the minimum value becomes -1. If the sign of the values changes over the curve either the maximum value becomes +1 or the minimum value becomes -1.

- **Range Normalization**

Here each row is divided by its range, i.e. “max value – min value”.

4.3 Derivative Methods and its applications

Derivative method is a preprocessing tool and it is applied to the reflectance spectra. Derivatives are applied to correct for baseline effects in spectra for the purpose of removing nonchemical effects and creating robust calibration models. Derivatives may also aid in resolving overlapped bands.

- **First derivative**

The first derivative of a spectrum is simply a measure of the slope of the spectral curve at every point. The slope of the curve is not affected by baseline offsets in the spectrum, and thus the first derivative is a very effective method for removing baseline offsets. However, peaks in raw spectra usually become zero-crossing points in first derivative spectra, which can be difficult to interpret.

- **Second derivative**

The second derivative is a measure of the change in the slope of the curve. In addition to ignoring the offset, it is not affected by any linear “tilt” that may exist in the data, and is therefore a very effective method for removing both the baseline offset and slope from a spectrum. The second derivative can help resolve nearby peaks and sharpen spectral features. Peaks in raw spectra change sign and turn to negative peaks with lobes on either side in the second derivative. Also, we can identify the wavelengths characteristic of deoxy-hemoglobin, oxy-hemoglobin, lipid and water respectively by applying second derivative method on the reflectance/absorbance spectra of the canine spectral dataset. The negative peaks obtained in the second derivative curve would give the wavelengths corresponding to the chromophores.

5. Data Analysis

In this section, we will be discussing the various algorithms that will be applied on the canine spectral data set in order to differentiate the malignant and benign spectra.

5.1 Support Vector Machines

Support Vector Machine (SVM) is a pattern recognition method that is used widely in data mining applications, and provides a means of supervised classification. SVM was originally developed for the linear classification of separable data, but is applicable to nonlinear data with the use of kernel functions.

SVM are used in machine learning, optimization, statistics, bioinformatics, and other fields that use pattern recognition. The algorithm used within *The Unscrambler 10.1* is based on code developed by Chih-Chung Chang and Chih-Jen Lin of the National Taiwan University. Hsu et al, 2009 [20].

SVM is a classification method which is based on statistical learning. For classification purposes, it constructs a hyperplane in a high dimensional space. As the linear function is not always able to model such a separation, data are mapped into a new feature space and a dual representation is used with the data objects represented by their dot product. To handle non-linear classification cases, a kernel based SVM was proposed. Kernel based SVM maps high dimensional data from the original feature space to the kernel space, after which they solve the equations in the kernel space linearly. The support vector is defined as the reduced training data from the kernel.

SVM has advantages over classification methods such as neural networks, as it has a unique solution, and has less tendency of over fitting when compared to other nonlinear classification methodologies. Of course, the model validation is the critical aspect in avoiding overfitting for any method. SVMs are effective for modeling of nonlinear data, and are relatively insensitive to variation in parameters. SVM uses an iterative training algorithm to achieve separation of different classes.

Two SVM classification types are available in *The Unscrambler 10.1* which is based on different means of minimizing the error function of the classification. C-SVC: also known as Classification SVM Type 1 and nu-SVC: also known as Classification SVM Type 2. In the c-SVM classification, a capacity factor, C , can be defined. The value of C should be chosen based on knowledge of the noise in the data being modeled. Its value can be optimized through cross-validation procedures. When using nu-SVM classification, the nu value must be defined. Nu serves as the upper bound of the fraction of errors and is the lower bound for the fraction of support vectors. Increasing nu will allow more errors, while increasing the margin of class separation. The kernel type to be used as a separation of classes can be chosen from the following four options:

- Linear
- Polynomial
- Radial basis function
- Sigmoid

The radial basis function is set as the default kernel because it is the simplest and can model systems of varying complexity. It is an extension of the linear kernel. If the number of variables is very large the data

do not need to be mapped to a higher dimensional space and the linear kernel function is preferred. If a polynomial kernel is chosen, the order of the polynomial must also be given.

In the *Unscambler version 10.1*, when an SVM model is created a new node is added in the project navigator with a folder for the data used in the model, and the results folder. The results folder has the following matrices:

- Confusion matrix
- Parameters
- Probabilities
- Prediction

The main result of the SVM is the confusion matrix, which indicates how many samples were classified in each class, and the prediction matrix, which indicates the classification determined for each sample in the training set [20].

5.2 Linear Discriminant Analysis

Linear Discriminant Analysis (LDA) is a classification method that provides a linear transformation of n -dimensional feature vectors into an m -dimensional space ($m < n$). LDA is a supervised classification method, as the categories to which objects are to be classified is known before the model is created. The objective of LDA is to determine the best fit parameters for classification of samples by a developed model. The model can then be used to classify unknown samples.

LDA is the simplest of all possible classification methods that are based on Bayes' formula. From Bayes' rule one develops a classification model assuming the probability distribution within all groups is known, and that the prior probabilities for groups are given, and sum to 100% over all groups. It is based on the normal distribution assumption and the assumption that the covariance matrices of the two (or more) groups are identical. This means that the variability within each group has the same structure. The only difference between groups is that they have different centers. LDA considers both within-group variance and between-group variance. The estimated covariance matrix for LDA is obtained by pooling covariance matrices across groups.

When the variability of each group does not have the same structure (unequal covariance matrix), the shape of the curve separating groups is not linear, and therefore quadratic discriminant analysis will

provide a better classification model. The distance of observations from the center of the groups can also be measured using the Mahalanobis distance.

LDA is used for classifying objects (samples, people, foods, etc.) into groups based on features that can be used to describe the objects. This could include developing classifications models for a library of products, good vs. bad quality product, or healthy vs. cancerous cells. A typical example related to classifying objects or, more generally, recognizing patterns is not a simple task for automated procedures, particularly when the objects are of biological interest. For example, identifying species, predicting species distributions or finding gene expression patterns that predict the risk of developing a particular type of tumor are generally difficult tasks. Data can be different analytical techniques related to chromatographic hyphenated techniques, like liquid chromatography with diode array detection (LC-DAD), where a set of UV-Vis spectra are used for classification. Data from any type of measurement, including spectroscopic data, imaging data, or generic data such as a table of physical properties of samples, can be used for classification, if those measurements have features which describe the objects. But for an LDA to be a well-posed problem, the number of objects in the calibration set should be larger than the number of variables. Often variable selection is used during model development when LDA is applied to spectral data.

In order to overcome the constraint of requiring more objects than features, we may use PCA-LDA which reduces the data dimensionality using PCA prior to running LDA. The number of components would still need to be less than the number of objects in each class. PCA-LDA makes use of a common projection space for all the classes. This option may be chosen for classification using spectral data by enabling it in the Options tab of the analysis dialog.

Discriminant analysis can be done in *The Unscrambler 10.1* using linear discriminant analysis, which is described in the following, or by partial least squares regression methods (PLS-DA). LDA can be done in many different ways and *The Unscrambler version 10.1* has options for Linear, Quadratic and Mahalanobis classifiers.

The linear method is used when the difference between two groups can be represented by a linear function. When a curved line separates the distance between groups, the quadratic method is effective. This is the case when the covariance matrices differ from group to group. Quadratic discriminant analysis may perform better in situations where the different groups being classified have their main variability in different directions, but only when the training sets used are large. The Mahalanobis distance is a way of measuring the distance of an observation to the centers of the groups, and uses ellipses to define the distances.

The results of the LDA classification are the predicted class for each sample, presented in the results matrix Prediction, and the matrix containing the Confusion matrix. The prediction matrix exhibits the probability of membership for each class, as well as the predicted class for each sample added as a category variable in the column Predicted. For an LDA to be performed, the number of samples within each category must be more than the number of variables.

5.3 Principal Component Analysis

Principal Component analysis is a mathematical variable reduction procedure, that converts a larger number of observed variables into a smaller number of variable (called principal components), that will take in account most of the variance in the observed variables. Number of original variables is more than or equal to the number of principal componnets. In this technique, the first principal component has the highest variance; the second principal component has the second highest variance and so on. But each principal component should be orthogonal to the one before that.

PCA helps us to identify pattern in data and emphasize on the similarities and differences of the dataset. When the data had a large number of variables, patterns in the dataset are difficult to be recognized. So PCA is a useful tool for analyzing data In this project, we can use PCA on the raw canine data, and also the normalized data to see if we get separate clusters of the benign, malignant and normal Region of Interests (ROI). We will be using the PCA plot tool in the *Unscrambler 10.1* for this purpose.

5.4 Tissue Optical Indices

A variety of optical indices have been developed in literature, that best correlate with the pathological state of breast tissue or with tissue density levels [13]. For example, tissue optical indices (TOI) aimed at enhancing contrast between cancerous and healthy tissue has been defined as follows:

$$TOI = \frac{[H_2O][HbT]}{[Lipid][StO_2]} \quad (1)$$

These measurements have underlying physiological meaning . Higher content of hemoglobin (HbT) suggests elevated tissue volume and angiogenesis; higher water content (H₂O) suggest edema and increased cellularity, decreased StO₂ indicated tissue hypoxia (a pathological condition in which tissue is deprived of adequate oxygen supply) driven by metabolically active tumor cells, decreased lipid content [Lipid] reflects displacement of parenchymal adipose. A higher TOI suggest that the tumor is malignant, because it indicates higher metabolic activity of the cells.

For this method, we need to find out the four wavelengths characteristic of the four tissue chromophores. Then we have to find a relationship between the two parameters: concentration and the reflectance intensity. This is because the above formula is in terms of concentration but our spectral data is in terms of reflectance intensity.

6. Preliminary Results

In this section, we discuss the preliminary results. The aim of these experiments is to demonstrate the potential of hyperspectral imaging system for mammary tumor characterization and discriminate benign and malignant mammary tumors. A total of 22 mammary tumors were used for the *in vivo* imaging study. Hyperspectral images were acquired from each canine patient. Quantitative analysis of the spectral images was performed to compare the spectra of cancer, benign and normal tissue.

As shown in Figure 9 and 10, the spectra of cancer tissue clearly differ from those of benign and normal tissue. It is interesting that the cancer tissue, within a single patient, has relatively low reflectance intensity compared to the benign and normal tissue, in the wavelength range between 650nm to 1100nm. . Previous studies have shown that cancerous tissues are associated with higher hemoglobin and water content, and lower lipid concentration with respect to benign tissue. The decreased reflectance intensity observed for malignant tumors is due to the increased microvasculature and therefore higher blood content of cancerous tissue relative to benign tissue.

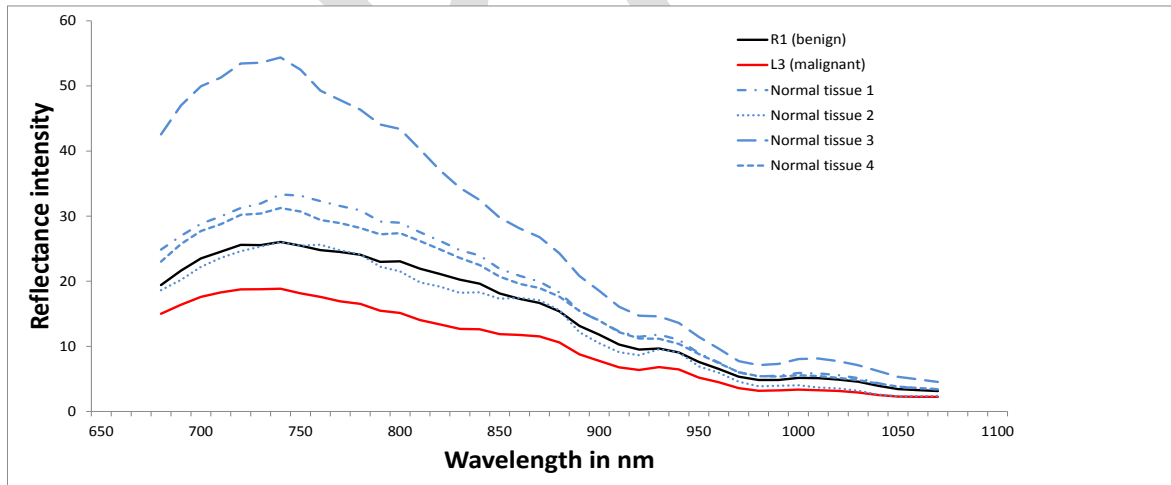


Figure 9: The reflectance spectra of canine patient Kiki. The malignant tumor has a lower reflectance intensity in the wavelength range 650-1100nm, which indicates increased absorption in this region. This correlates with the literature results discussed in the previous section.

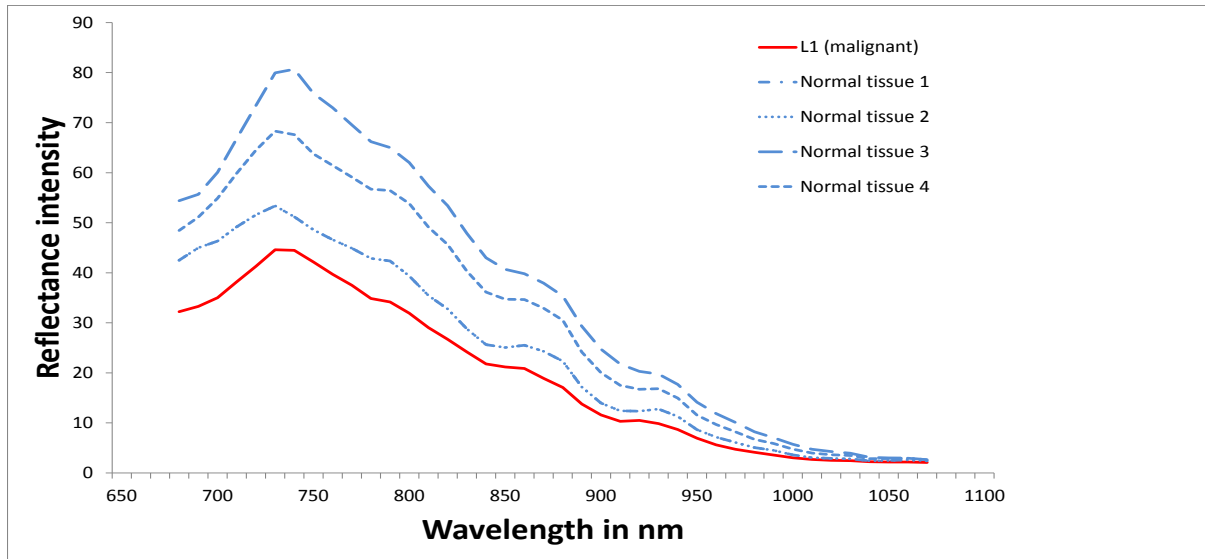


Figure 10: The reflectance spectra of canine patient Tinkerbell. The malignant tumor has a lower reflectance intensity in the wavelength range 650-1100nm, which indicates increased absorption in this region. This correlates with the literature results discussed in the previous section.

7. Discussion

In this study, we propose to use a hyperspectral imaging system for canine mammary cancer detection. The preliminary results are promising, and we see that within a single canine patient, we can differentiate the malignant and benign spectra based on the reflectance intensities. The malignant spectra has a lower reflectance intensity than the benign spectra over the NIR spectral range of 650-1100nm. This is due to the fact that the malignant tumors exhibit increased metabolic activity and thus the tissue concentration of oxy-hemoglobin and deoxy-hemoglobin is more in malignant tumors. Total hemoglobin concentration is directly related to blood volume. Since the blood volume of malignant tissue is more, the reflectance intensity value decreases.

There are a few issues that we faced during the hyperspectral imaging experiment of the mammary tumors of the canine patients. The lighting provided to the sample should be as uniform as possible. We used 500W white tungsten halogen lights to provide illumination. However, the temperature of the light is very high and it is uncomfortable for the patient to be under such high power light for a long time. In future experiments, we need to address this problem. Fiber optic cables can absorb some heat generated by the lights. So using a lamp to which a fiber optic cable is attached can be one approach to address the above issue. Also, the lamp that we are using at present is very large in size and not flexible. Using a lamp

with a fiber optic cable would increase the flexibility of the setup. Figure 11 shows the quartz tungsten halogen lamps that we are currently using. In future experiments, we can use the lightsources to which fiberoptic cable can be attached , as shown in Figure12.



Figure 11: The 500W quartz tungsten halogen lamp used in the canine experiment.

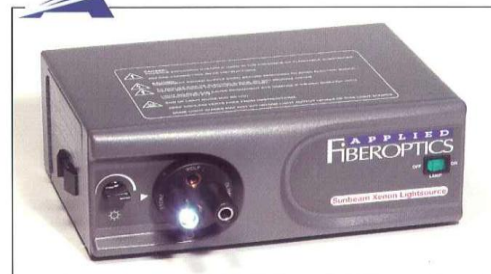


Figure 12: The 300W Sunbeam Xenon Lightsource to which a fiber optic cable can be attached.

Normalization of the data is also an important issue. Using the reflectance standards to normalize the data is the most common approach. The images of the reflectance standards should be taken under similar conditions and at the same time as the sample is imaged. However, during our data collection procedure, we did not use the standards. Therefore, we will investigate the best way to normalize the data using one of the software normalization methods. But in future experiments, we should definitely use the reflectance standards to normalize the data. Another aspect that needs to be discussed is the fact that the canine patients were not of uniform skin color. Some dogs had lighter skin color than the others. The skin color could be a problem during spectral analysis, because the lighter skin would automatically reflect more light than the darker skin.

The evolving imaging modality may have many potential applications in the medical field. In patients with cancer, if the cancer is diagnosed and treated early, the patient will have a better prognosis and a much greater chance of full recovery. HIS can be used not only for diagnosis, but also to determine the tumor margin. A safe resection margin can reduce operative mortality and morbidity, reduce the risk of complications and side effects, and therefore, yield greater long-term patient survival and a significantly more successful treatment outcome. Using HSI, a surgeon's visual capability is extended to invisible wavelengths. This technology expands the visual field from the three RGB spectral bands to more than a hundred spectral bands. As the large amount of data in hyperspectral images can be processed to broaden the spectral range, it can provide useful information for surgeons. HSI can also be used as a visual support tool during surgery. For example, by extending the visual field to infrared or far-infrared regions, previously invisible information can be exactly processed and then visually presented to a surgeon during an operation. Spectral data with a wealth of information can be automatically analyzed and quantified in order to aid in the identification of various tissue types. In this way, the imaging technique can extend a surgeon's visual field and thus help to continuously detect suspicious cancer tissues without interrupting the surgical procedure.

HSI also has the potential to detect important molecular biomarkers of cancer based on the unique spectral signature. Although the biochemical descriptions of the spectra are not known yet, it has been shown that the differences between the two spectra are caused by the mammary cancer having increased concentration of tissue water and hemoglobin and reduced concentration of lipid and StO₂. Tumor tissue displays decreased reflectance intensity in the 650-1100nm spectral range, corresponding to elevated tissue hemoglobin and water content. Higher content of hemoglobin suggests elevated tissue volume and angiogenesis; higher water content suggest edema and increased cellularity, decreased StO₂ indicated tissue hypoxia (a pathological condition in which tissue is deprived of adequate oxygen supply) driven by metabolically active tumor cells.

8. Future Research Plan

From the preliminary results obtained, we clearly see that there are spectral differences between the malignant, benign and normal Region of Interests (ROI). In future, we have to try out the different algorithms described in the Section 5, and find out which algorithm gives the best sensitivity and specificity.

To use the TOI method, we need to identify four wavelengths which are characteristic of deoxy-hemoglobin, oxy-hemoglobin, lipid and water. We can do this in two ways: Plot the absorption spectra to see if there are any peaks in the spectra which correspond to the four chromophores or plot the second derivative reflectance/absorbance spectra and then look for the negative peaks. To use the TOI method we have to find a relationship between the concentration of the chromophores and their reflectance intensities. This is because the equation for the TOI is in terms of concentration, but in our spectral dataset we have the reflectance values.

Also, as mentioned before, normalization of the data is very important for preparing the data for analysis. So we have to figure the best way to normalize the data using the methods discussed in Section 4.2.

To ensure repeatability of the hyperspectral sensor, we can conduct an experiment where the spectral image of a particular sample is taken in similar light conditions over 7 consecutive days, and the spectral plots are compared to check how repeatable the system is.

Also, we have to find out what are the minimum size tumors that our spectral system can detect. And also how deep into the tissue (depth of interrogation) the tumors can be detected.

References

- [1] "Mammary Tumors: Introduction". The Merck Veterinary Manual, 2006.
- [2] <http://www.caninecancer.com/mammary.html>
- [3] Akbari,Hamed, Halig,Luma V, Schuster, David M, Osunkoya, Adeboye, Master, Viraj, Nieh, Peter T, Chen, Georgia Z, Fei, Baowei, Hyperspectral imaging and quantitative analysis for prostate cancer detection, Journal of Biomedical Optics, 2012
- [4] Hamed Akbari¹, Kuniaki Uto, Yukio Kosugi, Kazuyuki Kojima, Naofumi Tanaka, Cancer detection using infrared hyperspectral imaging, Cancer Science, pp: 852-857, 2011.
- [5] Liu, Z.; Wang, H.; Li, Q. Tongue Tumor Detection in Medical Hyperspectral Images. Sensors 2012, 12, 162-174.
- [6] Medina JM, Pereira LM, Correia HT, Nascimento SM, Hyperspectral optical imaging of human iris

in vivo: characteristics of reflectance spectra, *J Biomed Opt*, 2011.

[7] Panasyuk SV, Yang S, Faller DV, Ngo D, Lew RA, Freeman JE, Rogers AE, Medical hyperspectral imaging to facilitate residual tumor identification during surgery, *Cancer Biol Ther*, pp:439-46, 2007

[8] Akbari H, Kosugi, Y. ; Kojima, K. ; Tanaka, N, Detection and Analysis of The Ischemia Using Visible and Invisible Hyperspectral Imaging, *IEEE Transactions of Biomedical Engineering*, pp. 2011-2017, August 2010.

[9] Cancio LC, Batchinsky AI, Mansfield JR, Panasyuk S, Hetz K, Martini D, Jordan BS, Tracey B, Freeman JE, Hyperspectral Imaging: A new Approach to the Diagnosis of hemorrhagic shock, *J Truama*, pp: 1087-95, 2006 .

[10] Jong-Ha Lee, Chang-Hee Won, "Characterization of Lung Tissues using Liquid-Crystal Tunable Filter an Hyperspectral Imaging System," *Proceedings of IEEE EMBC 09, 31th Annual International Conference of the IEEE Engineering in Medicine and Biology Society, Minneapolis, MN, September 6-9, 2009.*

[11] C. Balas, G. Themelis, A. Papadakis, E. Vasgiouraki, A. Argyros, E. Koumantakis, A Tosca, E. Helidonis, A Novel Hyper-Spectral Imaging System : Application on in-vivo Detection and Grading of Cervical Precancers and of Pigmented Skin Lesions, In *Proc. of "Computer Vision Beyond the Visible Spectrum" CVBVS'01 Workshop, Hawaii, USA, Dec. 2001.*

[12] A.F. H. Goetz, "Three decades of hyperspectral remote sensing of the earth: a personal view," *Remote Sens. Environ.* 113 (Suppl. 1), S5-S16, 2009

[13] Sergio Fantini and Angelo Sassaroli, Near-Infrared Optical Mammography for Breast Cancer, Detection with Intrinsic Contrast, *Annals of Biomedical Engineering*, Vol 40, No. 2, 2011, pp. 398-407.

[14] Shah, N., A. E. Cerussi, D. Jakubowski, D. Hsiang, J. Butler, and B. J. Tromberg, The role of diffuse optical spectroscopy in the clinical management of breast cancer. *Dis. Markers* 19:95–105, 2003.

- [15] A. Cerussi, N. Shah, D. Hsiang, J. Butler, B. J. Tromberg, In vivo absorption, scattering, and physiologic properties of 58 malignant breast tumors determined by broadband diffuse optical spectroscopy, *Journal of Biomedical Optics*, 11(4), 044005, 2006.
- [16] D. T. Dicker, J. Lerner, P. V. Belle, S. F. Barth, D. Guerry, M. Herlyn, D. E. Elder, W. S. El-Deiry, Differentiation of Normal Skin and Melanoma using High Resolution Hyperspectral Imaging, *Cancer Biology and Therapy*, 1033-1038, August 2006.
- [17] H. Akbari, Y. Kosugi, K. Kojima, N. Tanaka, Detection and Analysis of the Intestinal Ischemia Using Visible and Invisible Hyperspectral Imaging, *IEEE Transactions on Biomedical Engineering*, Vol 57, No. 8, August 2010.
- [18] A. Rinnan, F. Berg, S. Engelsen, Review of the most common pre-processing techniques for near-infrared spectra, *Trends in Analytical Chemistry*, Vol. 28, No. 10, 2009
- [19] B.J. Tromberg, N. Shah, R. Lanning, A. Cerussi, J. Espinoza, T. Pham, L. Svaasand and J. Butler, Non-invasive in vivo characterization of breast tumors using photon migration spectroscopy, *Neoplasia* 2 (2000), 26–40.
- [20] The Unscrambler 10.1 Software Manual.
- [21] M. Gurfinkel, A.B. Thompson, W. Ralston, T. L. Troy, A. L. Moore, T. A. Moore, J. Devens Gust, D. Tatman, J. S. Reynolds, B. Muggenburg, K. Nikula, R. Pandey, R. H. Mayer, D. J. Hawrysz and E. M. Sevick-Muraca, Pharmacokinetics of ICG and HPPH-car for the Detection of Normal and Tumor Tissue Using Fluorescence, Near-Infrared Reflectance Imaging: A Case Study, *Photochemistry and Photobiology*, 2000, 72(1), 94-102